

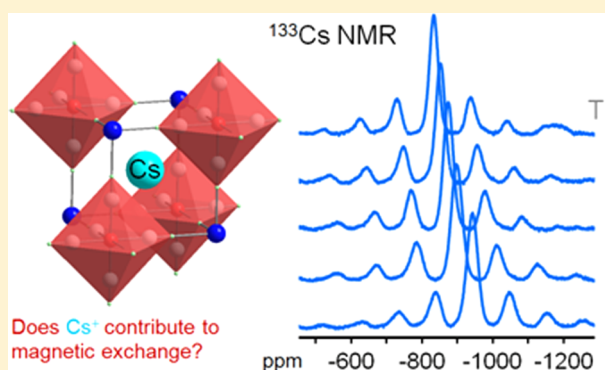
# Paramagnetic Prussian Blue Analogues $\text{CsM}^{\text{II}}[\text{M}^{\text{III}}(\text{CN})_6]$ . The Quest for Spin on Cesium Ions by Use of $^{133}\text{Cs}$ MAS NMR Spectroscopy

Frank H. Köhler\* and Oksana Storcheva

Department Chemie, Technische Universität München, 85748 Garching, Germany

**S** Supporting Information

**ABSTRACT:** The  $^{133}\text{Cs}$  magic-angle spinning NMR spectra of the paramagnetic compounds  $\text{CsM}^{\text{II}}[\text{M}^{\text{III}}(\text{CN})_6]$ ,  $\text{M}^{\text{II}} = \text{Ni}, \text{Co}, \text{Fe}, \text{Mn}$ ;  $\text{M}^{\text{III}} = \text{Co}, \text{Fe}$ , yield unusually large and temperature-dependent signal shifts (up to  $-950$  ppm relative to  $\text{CsCl}$  at 298 K). Comparison with the spectra of the diamagnetic analogues  $\text{CsM}[\text{Co}(\text{CN})_6]$ ,  $\text{M} = \text{Zn}, \text{Cd}$ , shows that the shifts are largely due to the unpaired electrons. This is ascribed to through-bond transfer of spin to the  $\text{Cs}^+$  ions, while the through-space effect of the magnetic moments on the signal shifts is shown to be virtually negligible. The mechanism inducing negative spin at  $\text{Cs}^+$  is discussed. The magnitude of the spin density (average:  $15.8 \times 10^{-3} | \text{a.u.} |^{-3}$ ) suggests that  $\text{Cs}^+$  is involved in magnetic exchange interactions of corresponding Prussian blue derivatives.



## INTRODUCTION

Do the putatively innocent alkali ions of paramagnetic Prussian blue analogues sense the unpaired electrons with potential impact on the overall magnetic behavior? The interest in this question becomes obvious when recalling some basic facts. The genuine Prussian blue,  $\text{Fe}^{\text{III}}_4[\text{Fe}^{\text{II}}(\text{CN})_6]_3(\text{H}_2\text{O})_x$ , is the eponym of polynuclear hexacyanometalates that have a cubic crystal structure.<sup>1</sup> The structure (cf. Figure 1) derives from the

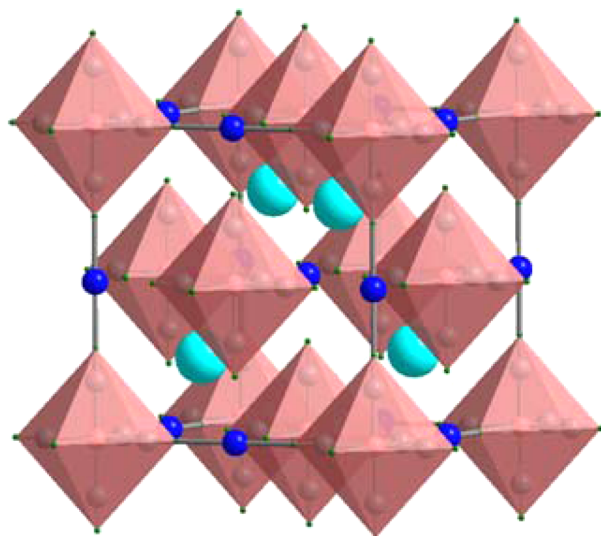


**Figure 1.** Idealized unit cell of the Prussian blue analogues  $\text{AM}^{\text{II}}[\text{M}^{\text{III}}(\text{CN})_6]$  (coordination spheres of the  $[\text{M}^{\text{III}}(\text{CN})_6]^{3-}$  octahedra completed), the alkali ions  $\text{A}^+$  are turquoise. Adapted from ref 2.

fact that  $\text{M}^{\text{III}}$  ions (blue, here  $\text{Fe}^{\text{III}}$ ) are coordinated by the nitrogen corners of six hexacyanometalate octahedra,  $[\text{M}^{\text{II}}(\text{CN})_6]^{n-}$  (dusky rose, here  $[\text{Fe}^{\text{II}}(\text{CN})_6]^{3-}$ ), and that hence the atom alignment  $\cdots\text{N}-\text{M}^{\text{III}}-\text{N}-\text{C}-\text{M}^{\text{II}}-\text{C}\cdots$  extends in three dimensions forming a supramolecular network. The charge difference of  $\text{M}^{\text{II}}$  and  $\text{M}^{\text{III}}$  may be compensated by alkali ions,  $\text{A}^+$  (turquoise), sitting in cubic holes of the lattice. An example is  $\text{MA}^{\text{II}}[\text{B}^{\text{III}}(\text{CN})_6]$  whose structure<sup>2</sup> is illustrated in Figure 1.

When  $\text{M}^{\text{II}}$  and  $\text{M}^{\text{III}}$  are paramagnetic transition metal ions this often entails intriguing magnetic characteristics such as ferri-<sup>3,4</sup> and ferromagnetism.<sup>4</sup> Spontaneous alignment of the electron spins can occur up to slightly more than  $100$  °C for Prussian blues containing alkali ions<sup>5,6</sup> and to  $42$ – $57$  °C without.<sup>6,7</sup> Hence these materials are known as room-temperature Prussian-blue magnets. Because of the promising properties and the prospect to design similar materials, theoretical concepts were developed. It has early been suggested that magnetic ordering can be effected by superexchange,<sup>8</sup> and this has been applied to Prussian blues.<sup>3,9</sup> Thus, the CN ligands function as mediators of the exchange interaction between the spins at the metal ions  $\text{M}^{\text{II}}$  and  $\text{M}^{\text{III}}$  whose distance would be too large to significantly contribute to the magnetic interaction without CN. The superexchange has been ascribed to two mechanisms: (i) some spin population exists at all atoms that share singly occupied molecular orbitals (MOs) containing the spin sources  $\text{M}^{\text{II}}$  and  $\text{M}^{\text{III}}$  (direct delocalization, positive spin throughout) and (ii) successive polarization of the paired electrons in  $\sigma$  bonds departing from

Received: April 2, 2015

Published: July 2, 2015

$M^{\text{II}}$  and  $M^{\text{III}}$  (spin polarization, alternating spin signs).<sup>10</sup> How efficient these mechanisms are is reflected in the signs of the spin density at the atoms that are involved. Experimentally, the resulting spin densities have been determined for the Prussian blues themselves or for appropriate model compounds by using polarized neutron diffraction (PND),<sup>11</sup> X-ray magnetic circular dichroism,<sup>12</sup> and electron paramagnetic resonance<sup>13</sup> as well as NMR<sup>14</sup> spectroscopies. The access to the spin densities is more or less direct, and the resolution varies, partly to the point of just qualitative results.<sup>12</sup> But it is clear that if  $M^{\text{III}}$  is the dominating spin source, the map of isotropic spin of the fragment  $\cdots M^{\text{II}}-N-C-M^{\text{III}}\cdots$  looks as shown in Figure 2, which reflects spin polarization. It has been amended by anisotropic components.<sup>11b-d,14b</sup>

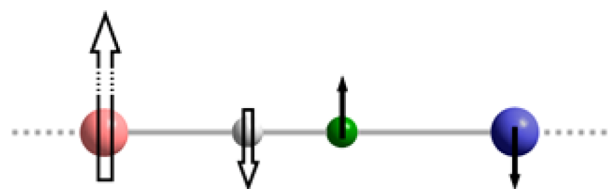


**Figure 2.** Qualitative distribution of isotropic spin in the Prussian blue fragment  $\cdots M^{\text{III}}-C-N-M^{\text{II}}\cdots$ .

Thus, while the NMR access to spin at the lattice atoms is now established, the next step would be to look into the interstices, in particular at the alkali ions therein. Therefore, we undertook an exploratory NMR study of some representative Prussian blue analogues  $AM^{\text{II}}[M^{\text{III}}(\text{CN})_6]$ .

## ■ BACKGROUND

If there is any spin density at the alkali ions  $A$  of  $AM^{\text{II}}[M^{\text{III}}(\text{CN})_6]$  the most suitable nucleus to detect it by NMR spectroscopy is  $^{133}\text{Cs}$ . Apart from lithium, which is not relevant for this type of compound,  $^{133}\text{Cs}$  has by far the smallest quadrupole moment (vide infra) of the alkali nuclei, and its NMR receptivity is close to the best value.<sup>15</sup> Also important is the fact that the parameter of interest, the spin density in the  $i$ th  $s$  orbital of some nucleus  $N$ ,  $\rho(N_{is})$ , is obtained from the isotropic contact shift of  $N$  at the temperature  $T$ ,  $\delta_{T,\text{iso}}^{\text{con}}(N)$ :<sup>16</sup>

$$\delta_{T,\text{iso}}^{\text{con}}(N) = \frac{\mu_0 g_e^2 \beta_e^2 (S + 1)}{9k_B T} \cdot \rho(N_{is}) \cdot F(g_{jj}, D) \quad (1)$$

The spin density depends on  $|\psi_{is}(0)|^2$  where  $\psi_{is}$  describes the relevant  $s$  orbital of  $N$ . In the series of alkali ions  $\text{Na}^+$ ,  $\text{K}^+$ ,  $\text{Rb}^+$ , and  $\text{Cs}^+$  the parameter  $|\psi_{is}(0)|^2$  amounts to 3.6, 5.0, 8.7, and  $11.3 \text{ \AA}^{-3}$ , respectively; when the next lower  $s$  orbitals are concerned (due to spin polarization) the numbers are 158, 129, 197, and  $220 \text{ \AA}^{-3}$ .<sup>17</sup> In any case, it is optimal for the cesium ion. As for the other parameters in eq 1,  $\mu_0$  is the magnetic constant,  $g_e$  is the electron  $g$  factor,  $\beta_e$  is the Bohr magneton,  $S$  is the electron spin quantum number, and  $k_B$  is the Boltzmann constant. In the following  $N = ^{133}\text{Cs}$ , and the label (N) will be partly dropped. The last term of eq 1 is a function of the  $g$  tensor values and the zero-field splitting  $D$ ; it is outlined in the Supporting Information.

## ■ RESULTS AND DISCUSSION

**Spectral Features.** A representative example is the  $S = 1$  compound  $\text{CsNi}[\text{Co}(\text{CN})_6]$ . Its  $^{133}\text{Cs}$  magic-angle spinning (MAS) NMR spectrum (Figure 3) shows a strongly shifted

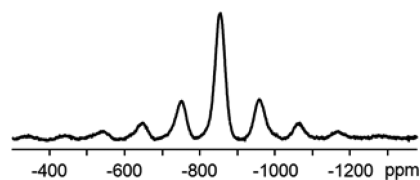


**Figure 3.**  $^{133}\text{Cs}$  MAS NMR spectrum of  $\text{CsNi}[\text{Co}(\text{CN})_6]$  at  $75^\circ\text{C}$ , spinning rate 4 kHz, shift scale relative to  $\text{CsCl}$ .

center band accompanied by spinning sidebands that span a range of  $\sim 30$  kHz. The signal is 530 ppm more shifted to low frequency than that of the diamagnetic analogue  $\text{CsZn}[\text{Co}(\text{CN})_6]$ , which is a clear indication that the  $\text{Cs}^+$  ion senses the paramagnetism of  $\text{CsNi}[\text{Co}(\text{CN})_6]$ . This is confirmed by the dependence of the signal shift on the temperature, which follows the Curie law; that is,  $|\delta| \approx 1/T$ <sup>16</sup> (Figure 4). The  $^{133}\text{Cs}$

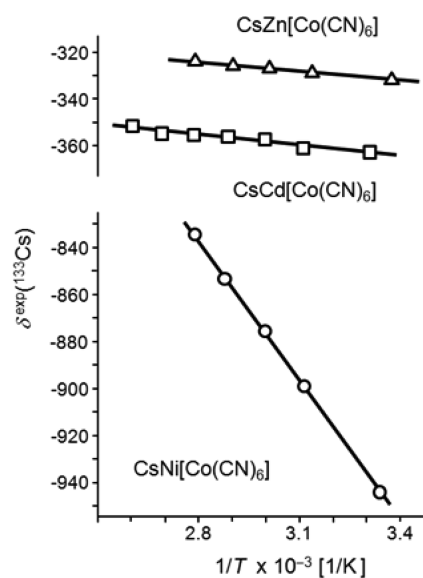


**Figure 4.** Temperature dependence of the  $^{133}\text{Cs}$  NMR signal shifts of  $\text{CsNi}[\text{Co}(\text{CN})_6]$ ,  $\text{CsZn}[\text{Co}(\text{CN})_6]$ , and  $\text{CsCd}[\text{Co}(\text{CN})_6]$  relative to that of  $\text{CsCl}$ .

MAS NMR spectra of  $\text{CsCo}[\text{Co}(\text{CN})_6]$ ,  $\text{CsFe}[\text{Co}(\text{CN})_6]$ , and  $\text{CsMn}[\text{Fe}(\text{CN})_6]$  are similar. In particular, due to the paramagnetism, the half widths of their center bands are  $\sim 2$  to 5 times larger than that of  $\text{CsZn}[\text{Co}(\text{CN})_6]$ , thus blurring any potential fine structure that might arise from quadrupole interaction and nonideal stoichiometry and symmetry. Details are listed in Table 1 below.

According to eq 1 the spin density is obtained from the contact shift, which is a component of the shift resulting from the paramagnetism  $\delta_T^{\text{para}}$ , which in turn is a component of the experimental shift (measured relative to the signal of solid  $\text{CsCl}$ )  $\delta_T^{\text{exp}}$ :<sup>16</sup>

$$\delta_T^{\text{exp}} = \delta_T^{\text{para}} + \delta^{\text{dia}} = \delta_T^{\text{con}} + \delta_T^{\text{dip}} + \delta^{\text{dia}} \quad (2)$$

The dipolar shift  $\delta_T^{\text{dip}}$  shall be considered below, while the diamagnetic shift, that is, the shift that the compound had if it were diamagnetic,  $\delta^{\text{dia}}$ , was taken from  $\text{CsZn}[\text{Co}(\text{CN})_6]$  and  $\text{CsCd}[\text{Co}(\text{CN})_6]$ . The diamagnetic shift is usually considered to be constant with temperature. But, surprisingly, in the present case it turned out to be temperature-dependent as well, although much less than that found for  $\text{CsNi}[\text{Co}(\text{CN})_6]$

**Table 1.**  $^{133}\text{Cs}$  Nuclear Magnetic Resonance Signal Shifts ( $\delta$  in ppm) and Signal Half Widths ( $\Delta$  in Hz) as well as Total Spin Densities ( $\rho$  in  $(\text{au})^{-3}$ ) at  $\text{Cs}^+$  of Selected Prussian Blue Analogues

compound	$S^a$	$\delta_{298}^{\text{exp } b}$	$\Delta_{298}$	$\delta_{298}^{\text{para } b}$	$\delta_{298}^{\text{dip } c}$	$\delta_{298}^{\text{con}}$	$\rho^{\text{total}} \times 10^{-5}$
$\text{CsNi}[\text{Co}(\text{CN})_6]$	1	-946	1500	-598	-0.4 + 0.5	$-599 \pm 16$	$-466 \pm 15$
$\text{CsCo}[\text{Co}(\text{CN})_6]$	3/2	-943	1900	-595	+31.0-33.0	$-596 \pm 32$	$-522 \pm 26$
$\text{CsFe}[\text{Co}(\text{CN})_6]$	2	-791	3450 <sup>d</sup>	-443	+14.0-15.0	$-443 \pm 16$	$-523 \pm 19$
$\text{CsMn}[\text{Co}(\text{CN})_6]$	5/2	-914 <sup>e,f</sup>	3550 <sup>e</sup>	-566 <sup>e</sup>	+0.1 <sup>e</sup> -0.1	$-567 \pm 16^g$	$-718 \pm 12$
$\text{CsMn}[\text{Fe}(\text{CN})_6]$	5/2, 1/2	-838	1200	-490	+2.5-2.7	$-490 \pm 16$	$-682 \pm 22$
$\text{CsZn}[\text{Co}(\text{CN})_6]$	0	-332	750				
$\text{CsCd}[\text{Co}(\text{CN})_6]$	0	-364	850				

<sup>a</sup>According to previous work.<sup>30,31</sup> <sup>b</sup>From fits of temperature-dependent data unless stated otherwise. <sup>c</sup>Calculated for an arbitrary  $\text{Cs}^+$  displacement of  $\theta = 54.7^\circ \pm 5^\circ$  (see text and Supporting Information). <sup>d</sup>At 324 K. <sup>e</sup>At 303 K. <sup>f</sup>Shoulder at -880 ppm. <sup>g</sup>Corrected with  $\delta_{303}^{\text{dia}} = -346.6$  (mean shift value of  $\text{CsZn}[\text{Co}(\text{CN})_6]$  and  $\text{CsCd}[\text{Co}(\text{CN})_6]$ ) and converted to 298 K according to the Curie law.

(Figure 4). A temperature-dependent signal shift of diamagnetic solids may be due to molecular oxygen in the lattice.<sup>18</sup> It is known that  $\text{O}_2$  adsorbed in Prussian blue analogues magnetically interacts with the host, although only at low temperature.<sup>19</sup> We therefore studied a sample of  $\text{CsCd}[\text{Co}(\text{CN})_6]$  prepared under purified dinitrogen, but the temperature dependence did not change in the relevant range (see Figure S2, Supporting Information). Other reasons that have been proposed or established, but which have not been investigated in this work, are migration in the lattice,<sup>20</sup> dynamic behavior,<sup>21</sup> and thermal changes of the crystal lattice constants,<sup>22</sup> which are known for Prussian blue analogues.<sup>23</sup> The temperature dependence of  $\delta^{\text{dia}}$  was taken into account for determining  $\delta_T^{\text{con}}$  (Experimental Section), and because the  $^{133}\text{Cs}$  signal shifts of the zinc and cadmium compounds differ by  $\sim 30$  ppm, the mean value was used for  $\delta_T^{\text{dia}}$ . It is worth noting that calculations might give diamagnetic shifts that are more appropriate,<sup>24</sup> but the temperature dependence would be a challenge.

According to X-ray diffraction studies<sup>2</sup> the  $\text{Cs}^+$  ions have a cubic environment, so the quadrupole interaction as well as the shift anisotropy are expected to vanish; a single  $^{133}\text{Cs}$  NMR signal should be seen. But actually, for all compounds a sideband pattern appears (e.g., Figure 1), which uncovers a lowering of the local  $\text{Cs}^+$  symmetry. The symmetry lowering may have several reasons: While Jahn-Teller distortion of the  $\text{M}^{\text{II}}(\text{NC})_6$  units would not apply to all examples, general issues are deviations from the ideal stoichiometry,<sup>25</sup> disorder of the  $\text{M}^{\text{II}}$  and  $\text{M}^{\text{III}}$  ions,<sup>26</sup> nonlinearity of the fragments  $\cdots\text{M}^{\text{II}}-\text{N}-\text{C}-\text{M}^{\text{III}}\cdots$ ,<sup>27</sup> and disorder of the  $\text{Cs}^+$  ions.<sup>28</sup> In these cases the distribution of different  $\text{Cs}^+$  sites in the crystal lattice should lead to detailed signal patterns similar to those of the  $^{13}\text{C}$ ,  $^{15}\text{N}$ , and  $^{113}\text{Cd}$  MAS NMR spectra of other hexacyanometalates.<sup>14b,c</sup> But so far, signal broadening has prevented further insight. Given the large shifts, a small signal splitting due to different  $\text{Cs}^+$  sites may be neglected as long as we focus on the spin transfer. However, the symmetry lowering might have an impact on the dipolar shift components, which in turn might dominate the overall paramagnetic shift and query any spin transfer to  $\text{Cs}^+$ .

**Dipolar Signal Shifts.** These shifts arise from through-space interactions between electron and nuclear magnetic moments. The observed nucleus (here  $^{133}\text{Cs}$ ) may interact with the unpaired electron spin density localized at  $\text{M}^{\text{II}}$  or  $\text{M}^{\text{III}}$  and at the C and N atoms. For molecules this is known as metal- and ligand-centered shifts, which have been reviewed thoroughly by Knorr.<sup>29</sup> The dipolar shift due to spin at the metal ions is given by the expression<sup>16</sup>

$$\delta_T^{\text{dip,M}} = \frac{\mu_0}{4\pi} \frac{\beta_e^2}{9k_B T} \sum_i \frac{3\cos^2 \theta_i - 1}{r_i^3} f_S(S, g, D) \quad (3)$$

Here  $r_i$  are the vectors joining  $\text{Cs}^+$  and the respective paramagnetic metal ions  $\text{M}_i$ ,  $\theta_i$  are the angles between  $r_i$  and the magnetic axis at M, and  $f_S(S, g, D)$  is a function of the electron spin quantum number  $S$ , the  $g$  tensor, and the zero-field splitting constant  $D$ . The other symbols were mentioned above.

According to eq 3, the dipolar shift depends on the structure of the compound. In the case of  $\text{CsM}^{\text{II}}[\text{M}^{\text{III}}(\text{CN})_6]$  the  $\text{Cs}^+$  ion occupies the center of an octant of the unit cell with edges  $\text{M}^{\text{III}}-\text{C}-\text{N}-\text{M}^{\text{II}}$ . Then, in eq 3, one gets  $\cos^2 \theta = 1/3$ , and the dipolar shift is zero. However, we saw above that the sideband patterns of the NMR spectra point to some lowering of the symmetry. Model calculations (Supporting Information) for some arbitrary distortion show that, actually, the dipolar shift is almost negligible except for  $\text{CsCo}[\text{Co}(\text{CN})_6]$  and  $\text{CsFe}[\text{Co}(\text{CN})_6]$  where  $\delta_{298}^{\text{dip}}(^{133}\text{Cs})$  is still less than 6% of the paramagnetic shifts,  $\delta_{298}^{\text{para}}(^{133}\text{Cs})$  (Table 1). Dipolar shifts may be uncovered by a  $1/T^2$  temperature dependence of the paramagnetic shifts.<sup>16</sup> In the present case they are too small to be observed in the given temperature range. This is mainly due to the rather large  $\text{Cs}-\text{M}$  distances, and consequently, arbitrary changes of the distance  $r$  have less impact than those of the angle  $\theta$  (Supporting Information).

When spin density is delocalized to p and d orbitals of nonmetal nuclei adjacent to  $\text{Cs}^+$  and to  $\text{Cs}^+$  itself "ligand-centered" dipolar shifts must be considered.<sup>16</sup> If any spin arrives at  $\text{Cs}^+$ , an s orbital would be concerned so that the dipolar shift can be neglected.<sup>16a</sup> Delocalization into the carbon p and nitrogen p orbitals does occur, but the amount is much less than at the metals.<sup>14</sup> The  $\text{Cs}-\text{C}$  and  $\text{Cs}-\text{N}$  distances are still large ( $>3.8 \text{ \AA}$ ),<sup>2</sup> while the deviation of the corresponding angles  $\theta$  from the lattice octant's diagonal is less than  $10^\circ$ .<sup>2</sup> It follows that the ligand-centered dipolar shifts can be neglected as well. Note that the dipolar shifts are smaller than the error due to the diamagnetic reference shift except for  $\text{CsCo}[\text{Co}(\text{CN})_6]$  (vide infra).

**Spin Transfer to the  $\text{Cs}^+$  Ion.** The isotropic spin density (in  $(\text{au})^{-3}$ ) delocalized from a given spin source to the cesium ion can be calculated with eq 4, which was adapted from previous work.<sup>16</sup>

$$\rho(\text{Cs}) = \frac{9k_B T a_0^3}{\mu_0 g_{\text{av}}^2 \beta_e^2 (S+1) F(g_j, D)} \delta_{298, \text{iso}}^{\text{con}} \quad (4)$$

Here  $a_0$  is the Bohr radius,  $g_{av}$  is the average experimental  $g$  factor, and the other parameters were mentioned above. The details of the calculations (Supporting Information) reveal that  $F(g_{jj}, D)$  adds less than 1% to  $\rho_{is}^{total}$  except for  $CsCo[Co(CN)_6]$  where it is 5.5%. In Table 1 the spin values are given without the contribution of  $F(g_{jj}, D)$ . The errors are due to the reference procedure and to the dipolar shift ( $CsCo[Co(CN)_6]$ ).

The spin density at  $Cs^+$  is negative in all cases. It follows that the spin delocalization must include one polarization step or an odd number of more such steps. The simplest case for discussing the delocalization is  $CsNi[Co(CN)_6]$  because only two unpaired electrons in the  $e_g$  orbitals of the  $Ni^{2+}$  ion are engaged. From their direct delocalization along the  $\sigma$  bonds of the  $\cdots Ni-N-C-Co \cdots$  fragments would lead to positive spin at all atoms on the lattice edges. This is illustrated in Figure 5 for

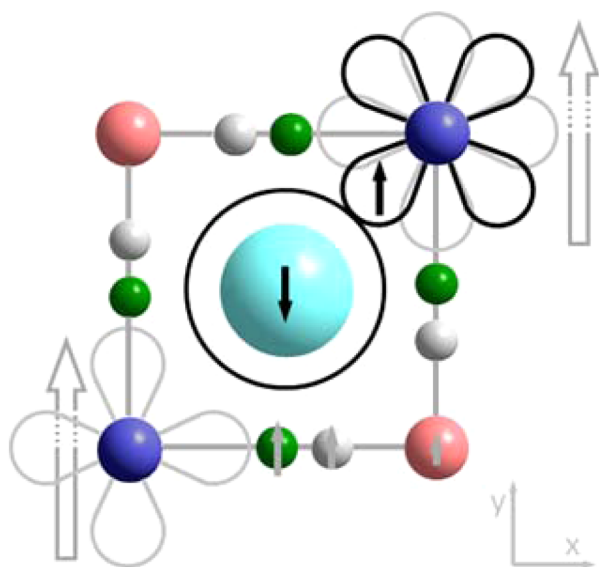


**Figure 5.** View on the top plane of a  $Cs^+$ -containing quadrant of  $CsNi[Co(CN)_6]$  showing spin delocalization. For clarity direct delocalization is only sketched along the bottom edge ( $\cdots Ni-N-C-Co \cdots$ , gray spin arrows) starting at the lower left  $Ni^{2+}$  ion. Spin polarization is only shown starting from the upper right  $Ni^{2+}$  ion (black spin arrows). See text for more details.

the  $\cdots Ni-N-C-Co \cdots$  fragment at the bottom. The singly occupied  $d_{x^2-y^2}$  orbital was selected, and the relevant spin arrows are gray. The  $Cs^+$  ion is located below the drawing plane, and the singly occupied  $e_g$  orbitals of the  $Ni^{2+}$  ion are oriented along the bonds rather than pointing to  $Cs^+$ . So any  $Cs$   $s$  orbital content in the spin-carrying MOs would be very small, and the transfer of positive spin is obviously overcompensated by spin polarization. It is worth noting that, by contrast, in  $Cs_2CuCl_4$  direct delocalization along  $\cdots Cu-Cl-Cs \cdots$  predominates and places positive spin on  $Cs^+$ .<sup>32</sup>

Spin polarization is conceivable to occur owing to overlap between a  $Cs$   $s$  and the  $Ni$   $t_{2g}$  orbitals. This is illustrated in Figure 5 where the upper right  $Ni^{2+}$  ion and its  $d_{xy}$  orbital (black contour) were singled out. The unpaired electron in the  $d_{x^2-y^2}$  orbital (gray contour) polarizes the paired electrons in the  $d_{xy}$  orbital such that the cesium nucleus senses some negative spin density. There are four  $Ni^{2+}$  ions with 12  $t_{2g}$  orbitals mediating the effect of eight unpaired electrons to one  $Cs^+$  ion, and yet the spin density at cesium is relatively small (vide infra).

This would be in accord with the expected weak interaction between the orbitals of cesium and nickel. The same reasoning applies to all other paramagnetic Prussian blue analogues listed in Table 1 because all have an  $e_g^2$  configuration. However, most compounds also have unpaired electrons in the  $t_{2g}$  orbitals (and at  $Fe^{3+}$  of  $CsMn[Fe(CN)_6]$ ), and it cannot be excluded that they modulate the spin density at cesium. Then additional parameters come into play and, at present, further discussion of the spin delocalization appears to be too speculative. That the spin delocalization to the alkali ions of hexacyanometalates may vary strongly can be seen from the PND study on  $Cs_2K[Cr(CN)_6]$ <sup>33</sup> where the spin density at  $Cs$  and  $K$  is  $-30 \times 10^{-5}$  and  $237 \times 10^{-5}$  (a.u.)<sup>-3</sup>, respectively. For  $CsMn[Cr(CN)_6]$  and  $CsNi[Cr(CN)_6]$  the magnetic moment at  $Cs$  (which reflects the spin density) was calculated to be very small and positive in both cases.<sup>34</sup>

Paramagnetic solids have been studied previously by  $^{133}Cs$  NMR spectroscopy (including Knight shift studies, which are a different topic). Examples are single-crystal studies of  $Cs_2CuCl_4$ ,<sup>32,35-37</sup>  $Cs_2CuBr_4$ ,<sup>32,38</sup>  $Cs_2CoCl_4$ ,<sup>32</sup>  $CsMnCl_3$ ,<sup>39</sup> and  $CsMnCl_3(H_2O)_2$ ,<sup>40</sup> static powder studies of  $Cs_2IrCl_6$ <sup>41</sup> and  $CsCo_6$ ,<sup>42</sup> and an MAS study of  $\alpha$ - $CsO_2$ .<sup>43</sup> Both positive and negative hyperfine couplings (partly given as hyperfine transferred fields) were claimed. Leading work has been published by Vachon et al.<sup>36,37</sup> Otherwise the hyperfine data were not corrected for the dipolar and the diamagnetic shift components of the experimental shifts although the latter may come to  $\sim 40\%$  (isotropic shifts of  $Cs_2ZnCl_4$  vs  $Cs_2CuCl_4$ <sup>32</sup>). The large negative  $^{133}Cs$  signal shift of  $\alpha$ - $CsO_2$  has been assumed to be purely dipolar,<sup>43</sup> whereas our own calculations establish predominating contact shifts (Supporting Information) and thus spin transfer from the  $O_2$  radical anion to  $Cs^+$ . Regarding other alkali ions, solid-state  $^6Li$  NMR is most rewarding. While there the focus is on the properties of lithium ion batteries, Grey et al.<sup>44</sup> have shown that it is the magnetism of these materials that enables an unusually high NMR resolution of local structural data. This is due to spin transfer to  $Li^+$  ions as has been established by the density functional theory calculations of Carlier et al.<sup>45</sup>

These findings invariably corroborate the present results: In Prussian blue analogues such as  $CsM^{II}[M^{III}(CN)_6]$  the  $Cs^+$  ions do receive spin density. There should thus be some contribution to the magnetic exchange interactions that follows the path  $\cdots M \cdots Cs \cdots M \cdots$ , at least when  $M$  has semioccupied  $e_g$ -type orbitals. The familiar exchange path is  $\cdots M^{III}-C-N-M^{II} \cdots$  (and/or vice versa) as mentioned above. Comparison of the average of the total isotropic spin densities at cesium with those at  $C$  and  $N$  of  $Cs_2K[Fe(CN)_6]$ <sup>14c</sup> and at  $M^{II}$  of  $CsCd[Fe(CN)_6]$  and  $Cd_3[Fe(CN)_6]_2$ <sup>14b</sup> reveals that at  $Cs^+$  it is not much smaller (between 2 and 6 times). Hence the importance of  $Cs^+$  for the magnetic exchange in Prussian blue analogues is worthy of being considered as well. In all probability, spin transfer to other ions occupying the quadrants of Prussian blue analogues and also to interstitial water can occur. The latter has actually been reported by Takeda<sup>46</sup> to give large  $^2H$  NMR signal shifts. Beyond the compounds of the present work  $^{133}Cs$  solid-state NMR spectroscopy is expected to be helpful for the study of similar materials, not least photomagnets.<sup>47</sup>

## EXPERIMENTAL SECTION

The samples were prepared as described by  $(CsMn[Fe(CN)_6])$  by analogy to) Griebler and Babel.<sup>30</sup> As for MAS NMR spectroscopy of paramagnetic compounds a general introduction has been given by

Pintacuda and Kervern.<sup>48</sup> The synthesized powders were freed from oxygen by repeated pumping down and refilling with purified dinitrogen before adding 3–5 wt % of (air-sensitive) nickelocene (as temperature sensor<sup>49</sup>) and packing the mixture into 4 mm ZrO<sub>2</sub> rotors sealed with Kel-F caps. To check whether residual O<sub>2</sub> in CsCd[Co(CN)<sub>6</sub>] was responsible for the temperature dependence of its <sup>133</sup>Cs signal, the sample was heated to 400 °C for 4 h in a Schlenk tube while branched to a high-vacuum pump. Subsequently, the sample was brought to ambient temperature, and the tube was filled with purified N<sub>2</sub>. The <sup>133</sup>Cs MAS NMR spectra were obtained from a Bruker Avance 300 spectrometer by applying nonselective single pulses and by subjecting the free induction decay to reverse linear prediction after eliminating the first data points, to exponential multiplication up to the matched filter, and to baseline correction. The decoupling channel was used to record the <sup>1</sup>H MAS NMR signal of the nickelocene for determining the internal temperature before and after each <sup>133</sup>Cs measurement. The temperature proved to be stable within ±0.5 °C.

All experimental chemical shifts at the temperatures  $T$ ,  $\delta_T^{\text{exp}}(^{133}\text{Cs})$ , were measured relative to that of CsCl powder. Second-order shift corrections were neglected because the quadrupole moment of <sup>133</sup>Cs is small and the Cs<sup>+</sup> sites are almost cubic, so the quadrupole coupling constants are expected to be also small.<sup>50</sup> The diamagnetic component of  $\delta_T^{\text{exp}}(^{133}\text{Cs})$  was obtained from powders of CsZn[Co(CN)<sub>6</sub>] and CsCd[Co(CN)<sub>6</sub>]. Their cesium signals varied with the temperature as  $\delta_T^{\text{dia}}(^{133}\text{Cs}) = (-13\,932/T) - 284.3$  and  $\delta_T^{\text{dia}}(^{133}\text{Cs}) = (-15\,464/T) - 311.9$ , respectively, so that, at the standard temperature, the shift was  $\delta_{298}^{\text{dia}}(^{133}\text{Cs}) = -331.1$  and  $-363.8$ , respectively. The center bands showed some structure, which has not been studied further, while the sidebands did not. Therefore, the cesium shift was derived from the first sidebands.

The paramagnetic shifts of the compounds CsM<sup>II</sup>[M<sup>III</sup>(CN)<sub>6</sub>] at given temperatures were calculated relative to CsZn[Co(CN)<sub>6</sub>] and CsCd[Co(CN)<sub>6</sub>] using the equations

$$\begin{aligned}\delta_T^{\text{para}}(^{133}\text{Cs}) &= \delta_T^{\text{exp}}(^{133}\text{Cs}) - \delta_T^{\text{dia}}(^{133}\text{Cs}) \\ &= \delta_T^{\text{exp}}(^{133}\text{Cs}) + (13\,932/T) + 284.3\end{aligned}$$

and

$$\begin{aligned}\delta_T^{\text{para}}(^{133}\text{Cs}) &= \delta_T^{\text{exp}}(^{133}\text{Cs}) - \delta_T^{\text{dia}}(^{133}\text{Cs}) \\ &= \delta_T^{\text{exp}}(^{133}\text{Cs}) + (15\,464/T) + 311.6\end{aligned}$$

From fits of the resulting shifts to 1/ $T$  the data at the standard temperature,  $\delta_{298}^{\text{para}}(^{133}\text{Cs})$ , were obtained (Table 1). The referencing procedure leads to an error of  $\delta_T^{\text{dia}}(^{133}\text{Cs}) = \pm 16$ .

## CONCLUSIONS

Paramagnetic Prussian blues of the type CsM<sup>II</sup>[M<sup>III</sup>(CN)<sub>6</sub>] yield <sup>133</sup>Cs MAS NMR spectra that indicate that the local symmetry of the Cs<sup>+</sup> ions is lower than the idealized cubic structure would suggest. On the way from the experimental signal shifts to spin densities diamagnetic and dipolar shift contributions must be eliminated. For the diamagnetic shift this is complicated by the fact that both the diamagnetic and the paramagnetic shifts are temperature-dependent. The dipolar shifts are negligibly small.

The remaining contact shifts can be converted to spin densities that are invariably negative. The negative sign may be explained by some interaction between a Cs *s* orbital and M<sup>II</sup> *t*<sub>2g</sub>-type orbitals and by polarization of the electron pairs therein through unpaired electrons in the M<sup>II</sup> *e*<sub>g</sub>-type orbitals. The amount of isotropic spin at Cs<sup>+</sup> is only ~2 times smaller than that at the N atoms of Cs<sub>2</sub>K[Fe(CN)<sub>6</sub>]. Hence magnetic exchange interaction in Prussian blues might also occur via Cs<sup>+</sup> (and other alkali ions) besides being mediated by CN ligand bridges. The results suggest that <sup>133</sup>Cs solid-state NMR

spectroscopy is beneficial for the study of related phenomena and other cesium-containing magnetic materials.

## ASSOCIATED CONTENT

### Supporting Information

<sup>133</sup>Cs MAS NMR spectra of CsCd[Co(CN)<sub>6</sub>] and CsZn[Co(CN)<sub>6</sub>], <sup>133</sup>Cs MAS NMR data of CsCd[Co(CN)<sub>6</sub>] with and without presence of dioxygen, <sup>133</sup>Cs dipolar signal shifts of CsM<sup>II</sup>[M<sup>III</sup>(CN)<sub>6</sub>], spin densities at Cs<sup>+</sup> of CsM<sup>II</sup>[M<sup>III</sup>(CN)<sub>6</sub>], and <sup>133</sup>Cs dipolar signal shifts of  $\alpha$ -CsO<sub>2</sub>. The Supporting Information is available free of charge on the ACS Publications website at DOI: 10.1021/acs.inorgchem.5b00711.

## AUTHOR INFORMATION

### Corresponding Author

\*E-mail: f.h.koehler@lrz.tu-muenchen.de

### Notes

The authors declare no competing financial interest.

## ACKNOWLEDGMENTS

This work was supported by the Deutsche Forschungsgemeinschaft, Priority Program 1137 entitled “Molecular Magnetism”.

## REFERENCES

- (1) Ludi, A.; Güdel, H. U. *Struct. Bonding (Berlin)* **1973**, *14*, 1–21.
- (2) Single crystal studies: (a) Dong, W.; Zhu, L.-N.; Song, H.-B.; Liao, D.-Z.; Jiang, Z.-H.; Yan, S.-P.; Cheng, P.; Gao, S. *Inorg. Chem.* **2004**, *43*, 2465–2467. (b) Coronado, E.; Giménez-López, M. C.; Levchenko, G.; Romero, F. M.; García-Boanza, V.; Millner, A.; Paz-Pasternak, M. *J. Am. Chem. Soc.* **2005**, *127*, 4580–4581. (c) Lu, Z.; Wang, X.; Liu, Z.; Liao, F.; Gao, S.; Xiong, R.; Ma, H.; Zhang, D.; Zhu, D. *Inorg. Chem.* **2006**, *45*, 999–1004. (d) Tokoro, H.; Shiro, M.; Hashimoto, K.; Ohkoshi, S.-I. *Z. Allg. Anorg. Chem.* **2007**, *633*, 1134–1136. (e) Vertelman, E. J. M.; Lummen, T. T. A.; Meetsma, A.; Bouwkamp, M. W.; Molnar, G.; van Loosdrecht, P. H. M.; van Koningsbruggen, P. J. *Chem. Mater.* **2008**, *20*, 1236–1238.
- (3) Babel, D. *Comments Inorg. Chem.* **1986**, *5*, 285–320.
- (4) (a) Dunbar, K. R.; Heintz, R. A. *Prog. Inorg. Chem.* **1997**, *49*, 283–391. (b) Verdager, M.; Girolami, G. *Magnetism: Molecules to Materials V*; Müller, J. S., Drillon, M., Eds.; Wiley-VCH: Weinheim, Germany, 2005, Vol. 5, pp 283–346.
- (5) Hatlevik, Ø.; Buschmann, W. E.; Zhang, J.; Mamson, J.; Miller, J. S. *Adv. Mater.* **1999**, *11*, 914–918.
- (6) Holmes, S. M.; Girolami, G. S. *J. Am. Chem. Soc.* **1999**, *121*, 5593–5594.
- (7) Ferlay, S.; Mallah, T.; Quahès, R.; Veillet, P.; Verdager, M. *Nature* **1995**, *378*, 701–703.
- (8) Anderson, P. W. *Phys. Rev.* **1959**, *115*, 2–13. Ginsberg, P. *Inorg. Chim. Acta Rev.* **1971**, *5*, 45–68.
- (9) Weihe, H.; Güdel, H. U. *Comments Inorg. Chem.* **2000**, *22*, 75–103.
- (10) (a) Cano, J.; Ruiz, E.; Alvarez, S.; Verdager, M. *Comments Inorg. Chem.* **1998**, *20*, 27–56. (b) Ruiz, E.; Cirera, J.; Alvarez, S. *Coord. Chem. Rev.* **2005**, *249*, 2649–2660.
- (11) (a) Brown, P. J.; Fischer, P.; Güdel, H. U.; Herren, F.; Ludi, A. *J. Phys. C* **1982**, *43*, 235–240. (b) Figgis, B. N.; Forsyth, J. B.; Reynolds, P. A. *Inorg. Chem.* **1987**, *26*, 101–105. (c) Daul, C. A.; Day, P.; Figgis, B. N.; Güdel, H. U.; Herren, F.; Ludi, A.; Reynolds, P. A. *Proc. R. Soc. London, Ser. A* **1988**, *419*, 205–219. (d) Figgis, B. N.; Kucharski, E. S.; Vrtis, M. *J. Am. Chem. Soc.* **1993**, *115*, 176–181. (e) Day, P.; Delfs, C. D.; Figgis, B. N.; Reynolds, P. A.; Tasset, F. *Mol. Phys.* **1993**, *78*, 769–780. (f) Stride, J. A.; Gillon, B.; Goukassov, A.; Larionova, J.; Clérac, R.; Kahn, O. *C. R. Acad. Sci., Ser. IIC: Chim.* **2001**, *4*, 105–112.
- (12) (a) Verdager, M.; Mallah, T.; Hélar, C.; L’Hermite, F.; Sainctavit, P.; Arrio, M. A.; Babel, D.; Baudalet, F.; Dartyge, E.; Fontaine, A. *Phys. B* **1995**, *208–209*, 765–767. (b) Dujardin, E.;

- Ferlay, S.; Phan, X.; Desplanches, C.; Cartier dit Moulin, C.; Sainctavit, P.; Baudelet, F.; Dartyge, E.; Veillet, P.; Verdagner, M. *J. Am. Chem. Soc.* **1998**, *120*, 11347–11352. (c) Champion, G.; Escax, V.; Cartier dit Moulin, C.; Bleuzen, A.; Villain, F.; Baudelet, F.; Dartyge, E.; Verdagner, M. *J. Am. Chem. Soc.* **2001**, *123*, 12544–12546.
- (13) Wolberg, A. *J. Chem. Phys.* **1971**, *54*, 1428–1430.
- (14) (a) Köhler, F. H.; Lescouëzec, R. *Angew. Chem., Int. Ed.* **2004**, *43*, 2571–2573. (b) Flambard, A.; Köhler, F. H.; Lescouëzec, R.; Revel, B. *Chem.—Eur. J.* **2011**, *17*, 11567–11575. (c) Baumgärtel, N.; Flambard, A.; Köhler, F. H.; Lescouëzec, R. *Inorg. Chem.* **2013**, *52*, 12634–12644 Scaled spin densities are given there. They must be multiplied by  $(S + 1)$  for the comparison with the total spin densities of the present work.
- (15) Harris, R. K.; Becker, E. D.; Cabral de Menzes, S. M.; Goodfellow, R.; Granger, P. *Pure Appl. Chem.* **2001**, *73*, 1795–1818.
- (16) (a) Kurland, R. J.; McGarvey, B. R. *J. Magn. Reson.* **1970**, *2*, 286–301. (b) *NMR of Paramagnetic Molecules*; La Mar, G. N., Horrocks, W. D., Holm, R. H., Eds.; Academic Press: New York, 1973. (c) Bertini, I.; Luchinat, C. In *Physical Methods for Chemists*; Drago, R. S., Ed.; Saunders College Publishing: Ft. Worth, TX, 1992; pp 500–556. (d) Bertini, I.; Luchinat, C.; Parigi, G. *Solution NMR of Paramagnetic Molecules. Applications to Metallobiomolecules and Models*; Elsevier: Amsterdam, The Netherlands, 2001.
- (17) Koh, A. K.; Miller, D. J. *At. Data Nucl. Data Tables* **1985**, *33*, 235–253.
- (18) (a) Liu, H.; Grey, C. P. *Microporous Mesoporous Mater.* **2002**, *53*, 109–120. (b) Accardi, R. J.; Lobo, R. F.; Kalwei, M. *J. Phys. Chem. B* **2001**, *105*, 5883–5886.
- (19) Kaye, S. S.; Choi, H. J.; Long, J. R. *J. Am. Chem. Soc.* **2008**, *130*, 16921–16925.
- (20) (a) Nagel, R.; Groß, Th. W.; Günther, H.; Lutz, H. D. *J. Solid State Chem.* **2002**, *165*, 303–311. (b) Kim, N.; Stebbins, J. F. *Chem. Mater.* **2009**, *21*, 309–315. (c) Bräunling, D.; Pecher, O.; Trots, D. M.; Senyshyn, A.; Zhereptsov, D. A.; Haarmann, F.; Niewa, R. *Z. Anorg. Allg. Chem.* **2010**, *636*, 936–946.
- (21) Soleilhavoup, A.; Hampson, M. R.; Clark, S. J.; Evans, J. S. O.; Hodgkinson, P. *Magn. Reson. Chem.* **2007**, *45*, S144–S155.
- (22) (a) Takahashi, T.; Kawashima, H.; Sugisawa, H.; Baba, T. *Solid State NMR* **1999**, *15*, 119–123. (b) Rossano, S.; Mauri, F.; Pickard, C. J.; Farnan, I. *J. Phys. Chem. B* **2005**, *109*, 7245–7250.
- (23) (a) Goodwin, A. L.; Chapman, K. W.; Kepert, C. J. *J. Am. Chem. Soc.* **2005**, *127*, 17980–17981. (b) Chapman, K. W.; Chupas, P. J.; Kepert, C. J. *J. Am. Chem. Soc.* **2006**, *128*, 7009–7014. (c) Matsuda, T.; Tokoro, H.; Hashimoto, K.; Ohkoshi, S.-I. *Dalton Trans.* **2006**, 5046–5050. (d) Matsuda, T.; Kim, J. E.; Ohoyama, K.; Moritomo, Y. *Phys. Rev. B* **2009**, *79*, 172302. (e) Adak, S.; Daemen, L. L.; Hartl, M.; Williams, D.; Summerhill, J.; Nakotte, H. *J. Solid State Chem.* **2011**, *184*, 2854–2861.
- (24) Kaupp, M.; Köhler, F. H. *Coord. Chem. Rev.* **2009**, *253*, 2376–2386.
- (25) Reference 4b, Chapter 9.2.2.
- (26) Nakamura, S.; Fuwa, A. *Hyperfine Interact.* **2014**, *226*, 267–274.
- (27) (a) Ferlay, S.; Mallah, T.; Ouahès, R.; Veillet, P.; Verdagner, M. *Inorg. Chem.* **1999**, *38*, 229–234. (b) Hallmeier, K. H.; Sauter, S.; Szargan, R. *Inorg. Chem. Commun.* **2001**, *4*, 153–156. (c) Bleuzen, a.; Escax, V.; Ferrier, A.; Villain, F.; Verdagner, M.; Münsch, P.; Itié, J.-P. *Angew. Chem., Int. Ed.* **2004**, *43*, 3728–3731. (d) Rodríguez-Hernández, J.; Reguera, E.; Lima, E.; Balmaseda, J.; Martínez-García, R.; Yee-Madeira, H. *J. Phys. Chem. Solids* **2007**, *68*, 1630–1642. (e) Her, J.-H.; Stephens, P. W.; Kareis, C. M.; Moore, J. G.; Min, S. K.; Park, J.-W.; Bali, G.; Kennon, B. S.; Miller, J. S. *Inorg. Chem.* **2010**, *49*, 1524–1534.
- (28) Papanikolaou, D.; Margadonna, S.; Kosaka, W.; Ohkoshi, S.-I.; Brunelli, M.; Prassides, K. *J. Am. Chem. Soc.* **2006**, *128*, 8358–8363.
- (29) Knorr, R.; Hauer, H.; Weiss, A.; Polzer, H.; Ruf, F.; Löw, P.; Dvortsák, P.; Böhrer, P. *Inorg. Chem.* **2007**, *46*, 8379–8390.
- (30) Griebler, W.-D.; Babel, D. *Z. Naturforsch., B* **1982**, *37*, 835–837.
- (31) Ishiji, K.; Deguchi, M.; Kawakami, K.; Nakajima, N.; Matsuda, T.; Tokoro, H.; Ohkoshi, S.-I.; Iwazumi, T. *J. Phys. Soc. Jpn.* **2010**, *79*, 074801.
- (32) Hartmann, H.; Strehlow, W.; Haas, H. *Z. Naturforsch., A* **1968**, *23*, 2029–2034.
- (33) Figgis, B. N.; Forsyth, J. B.; Reynolds, P. A. *Inorg. Chem.* **1987**, *26*, 101–105.
- (34) Eyert, V.; Siberchicot, B.; Verdagner, M. *Phys. Rev. B* **1997**, *56*, 8959–8969.
- (35) Lim, A. R.; Hong, K. S.; Jeong, S.-Y. *J. Phys. Chem. Solids* **2004**, *65*, 1373–1378.
- (36) Vachon, M.-A.; Kundhikanjana, W.; Straub, A.; Mitrović, V. F.; Reyes, A. P.; Kuhns, P.; Coldea, R.; Tylczinski, Z. *New. J. Phys.* **2006**, *8*, 222.
- (37) Vachon, M.-A.; Koutroulakis, G.; Mitrović, V. F.; Reyes, A. P.; Kuhns, P.; Coldea, R.; Tylczinski, Z. *J. Phys.: Condens. Matter* **2008**, *20*, 295225.
- (38) Fujii, Y.; Nakamura, T.; Kikuchi, H.; Chiba, M.; Goto, T.; Matsubara, S.; Kodama, K.; Takigawa, M. *Phys. B* **2004**, *346–347*, 45–49.
- (39) Lim, A. R.; Choh, S. H.; Jeong, S.-Y. *Solid State Commun.* **1996**, *99*, 19–22.
- (40) Lim, A. R.; Choh, S. H.; Jeong, S.-Y. *Phys. Status Solidi B* **1997**, *200*, 229–237.
- (41) Raaen, A. M.; Svare, I.; Pedersen, B. *Phys. B* **1983**, *121*, 89–94.
- (42) Tycko, R.; Dabaghi, G.; Murphy, D. W.; Zhu, Q.; Fischer, J. E. *Phys. Rev. B* **1993**, *48*, 9097–9105.
- (43) Krawietz, T. R.; Murray, D. K.; Haw, J. F. *J. Phys. Chem. A* **1998**, *102*, 8779–8785.
- (44) (a) Grey, C. P.; Lee, Y. J. *Solid State Sci.* **2003**, *5*, 883–894. (b) Grey, C. P.; Dupré, N. *Chem. Rev.* **2004**, *104*, 4493–4512.
- (45) Carlier, D.; Ménétrier, M.; Grey, C. P.; Demas, C.; Ceder, G. *Phys. Rev. B* **2003**, *67*, 174103.
- (46) Ishiyama, H.; Maruta, G.; Kobayashi, T.; Takeda, S. *Polyhedron* **2003**, *22*, 1981–1987.
- (47) (a) Hashimoto, K.; Ohkoshi, S.-I. *Philos. Trans. R. Soc. London, A* **1999**, *357*, 2977–3003. (b) Ohkoshi, S.-I.; Hashimoto, K. *J. Photochem. Photobiol. C* **2001**, *2*, 71–88. (c) Varret, F.; Bleuzen, A.; Boukheddaden, K.; Bousseksou, A.; Codjovi, E.; Enachescu, C.; Goujon, A.; Linares, J.; Menendez, N.; Verdagner, M. *Pure Appl. Chem.* **2002**, *74*, 2159–2168. (d) Sato, O. *J. Photochem. Photobiol. C* **2004**, *5*, 203–223. (e) Herrera, J. M.; Bachschmidt, A.; Villain, F.; Bleuzen, A.; Marvaux, V.; Wernsdorfer, W.; Verdagner, M. *Philos. Trans. R. Soc. London, A* **2008**, *366*, 127–138. (f) Tokoro, H.; Ohkoshi, S.-I. *Dalton Trans.* **2011**, *40*, 6825–6833.
- (48) Pintacuda, G.; Kervin, G. In *Topics in Current Chemistry. Modern NMR Methodology*; Heise, S., Matthews, S., Eds.; Springer: Berlin, Germany, 2013, Vol. 335, pp 157–200. Pell, A. J.; Pintacuda, G. *Prog. NMR Spectrosc.* **2015**, *84–85*, 33–72.
- (49) (a) Köhler, F. H.; Xie, X. *Magn. Reson. Chem.* **1997**, *35*, 487–492. (b) Heise, H.; Köhler, F. H.; Xie, X. *J. Magn. Reson.* **2001**, *150*, 198–206.
- (50) (a) Freude, D.; Haase, J. *NMR. Basic Principles and Progress*; Diehl, P., Fluck, E.; Günther, H., Kosfeld, R., Seelig, J., Eds.; Springer: Berlin, Germany, 1993; Vol. 29, pp 1–90. (b) Bräuninger, T.; Jansen, M. *Z. Anorg. Allg. Chem.* **2013**, *639*, 857–879.